

# Selection of *p*-nitrophenyl fatty acid substrate suitable for detecting changes in soil esterase activity associated with degradation of biodegradable polyester mulch films: A field trial

Shun Tsuboi,<sup>1</sup> Kimiko Yamamoto-Tamura,<sup>1</sup> Atsushi Takada,<sup>2</sup> Seiichiro Yonemura,<sup>1</sup> Yuko Takada Hoshino,<sup>1</sup> Hiroko Kitamoto,<sup>1</sup> Ayaka Wenhong Kishimoto-Mo<sup>1</sup>

<sup>1</sup>Institute for Agro-Environmental Sciences, National Agriculture and Food Research Organization (NARO), Tsukuba; <sup>2</sup>Kanagawa Agricultural Technology Center, Hiratsuka, Japan

## Highlights

- Biodegradable poly(butylene succinate-co-adipate) and two commercial films had different field degradation rates.
- Five *p*-nitrophenyl (*p*NP) fatty acid substrates were investigated to evaluate esterase activity in the soils.
- Three *p*NP substrates with shorter acyl chains could stably indicate an increase in hydrolytic activity with film degradation.
- In these substrates, the hydrolytic activities of *p*NP-acetate and -hexanoate were related to soil temperature and moisture, respectively.
- The hydrolytic activity of *p*NP-butyrate was a suitable indicator of the microbial activity associated with the film degradation.

Correspondence: Kimiko Yamamoto-Tamura, Institute for Agro-Environmental Sciences, National Agriculture and Food Research Organization (NARO), 3-1-3 Kannondai, Tsukuba, Ibaraki, 305-8604, Japan. Tel.: +81.29.838.8355. E-mail: kimtam@affrc.go.jp

Key words: Biodegradable polyesters; mulch films; cultivated field; soil esterase activity; *p*-nitrophenyl fatty acids.

Acknowledgements and funding: this study was financially supported by the research programme on the development of innovative technology grants (JPJ007097) from the Project of the Bio-oriented Technology Research Advancement Institution (BRAIN). The authors are grateful to Mr. Ken Suzuki for the NMR composition analysis of the biodegradable polymers in the commercial mulch films. Mr. Hideo Matsumoto for assistance with measurements of esterase activity in soils, and Ms. Yasuko Yotsui and Ms. Yoko Nakano for assistance with handling and preparing mesh bags entering the biodegradable films.

Contributions: the authors contributed equally to work and are listed in alphabetic order.

Received for publication: 17 January 2022.

Revision received: 30 April 2022.

Accepted for publication: 1 May 2022.

©Copyright: the Author(s), 2022

Licensee PAGEPress, Italy

Italian Journal of Agronomy 2022; 17:2040

doi:10.4081/ija.2022.2040

This article is distributed under the terms of the Creative Commons Attribution Noncommercial License (by-nc 4.0) which permits any non-commercial use, distribution, and reproduction in any medium, provided the original author(s) and source are credited.

Publisher's note: All claims expressed in this article are solely those of the authors and do not necessarily represent those of their affiliated organizations, or those of the publisher, the editors and the reviewers. Any product that may be evaluated in this article or claim that may be made by its manufacturer is not guaranteed or endorsed by the publisher.

## Abstract

This study aimed to develop a method for detecting microbial activity based on soil esterase activity during the biodegradation of polyester biodegradable mulch films after ploughing the field. Herein, we report that the *p*-nitrophenyl butyrate (*p*NP-C4) substrate, among five *p*NP fatty acid substrates [*p*NP-acetate (C2), -C4, -hexanoate (C6), -decanoate (C10), and -dodecanoate (C12)] in a cultivated field, is a specific indicator for detecting microbial activity associated with biodegradation of biodegradable polyesters. To evaluate film degradation by loss of weight and visual area, pieces of three different films were placed independently in meshed plastic bags and buried in a cultivated field in Japan for seven months. One was made from poly(butylene succinate-co-adipate) (PBSA), and two were (poly(butylene terephthalate-co-adipate) and poly(butylene succinate)-type polymer)-based commercial biodegradable mulch films (hereafter described as films A and B) and weathered for three months in the cultivated field. The soil adhered to the mesh bag and film was retrieved and mixed, and their esterase activities were measured using the five *p*NP fatty acid substrates. From the loss of visual area, the time taken from burial to accelerated degradation increased, in the order of PBSA, film A, and film B. The reproducibility of the hydrolytic activity values of *p*NP-C2, -C4, and -C6 in bulk soil were considered sufficient to measure baselines for the enzymatic activities. Among these substrates, the hydrolytic activity of *p*NP-C4 was significantly higher in the degradation process of PBSA and film A. In addition, unlike the *p*NP-C2 and -C6, the hydrolytic activity of the *p*NP-C4 in the bulk soil was not affected by changes in soil temperature and moisture under the conditions of this experiment. Therefore, the *p*NP-C4 hydrolytic activity can aid in the detection of the microbial activity associated with the biodegradation of polyester-based biodegradable mulch films in cultivated field soils.

## Introduction

Plastic mulching films are generally made with non-biodegradable polyethylene (PE) to maintain soil temperature and water retention and prevent soil erosion and weed growth. They contributed to improving yields and reduction of agrochemicals.

Unfortunately, such PE films are left behind on harvested fields, and retrieving them from soils is labouring for farmers. The used films are treated as industrial wastes, and their disposal requires a collection fee. The remaining PE fragments dispersed into the environment are poorly biodegradable, then they cause plastic pollution for a substantial period.

Biodegradable mulch films (BDMs) can replace non-biodegradable plastic mulch films that maintain soil moisture (Kader *et al.*, 2017) and suppress weed occurrence (Martín-Closas *et al.*, 2017). In addition, the BDMs can be degraded by microorganisms in soils after use (Bondopadhyay *et al.*, 2018). Thus, BDMs can reduce farmers' labour and waste disposal costs (Ngouajio *et al.*, 2008) and have been recognised as useful agricultural materials.

However, the residual BDMs from incomplete degradation can be responsible for reducing water retention and infiltration as well as non-BDMs in agricultural soils (Li *et al.*, 2014; Miles *et al.*, 2017). Hence, the standard criterion for aerobic biodegradability of plastics in soils (ISO 17556), which was first established in 2003 and updated in 2019 (Third Edition), is used to evaluate the biodegradability of BDMs in soils by measuring CO<sub>2</sub> generation. There have been many studies regarding the evaluation of the degradation potential of BDMs based on loss of visual area (Li *et al.*, 2014; Moreno *et al.*, 2017; Sintim *et al.*, 2020), mechanical resistance, such as puncture and tensile strength (Briassoulis, 2007; Moreno *et al.*, 2017), and analysis of the chemical changes of the BDMs (Hayes *et al.*, 2017; Sintim *et al.*, 2020) in soils of cultivated fields. However, these are not direct evidence of 'biodegradation' by soil microorganisms (Zumstein *et al.* 2019). Moreover, techniques based on the measurement of soil CO<sub>2</sub> emissions are unsuitable for agricultural fields because CO<sub>2</sub> emissions are difficult to detect. Moreover, it is still impractical to independently quantify heterotrophic respiration and the CO<sub>2</sub> release by BDM degradation in field trials (Francioni *et al.*, 2022). There are currently no standardised evaluation methods for the biodegradation of BDMs in soils of each cultivated field.

Enzymatic activity is one of the indicators of the metabolic activity of soil microorganisms. Commercial BDMs contain several compounds, such as starch, cellulosic fibre, polylactic acids, and aliphatic/aromatic *co*-polymers (Martín-Closas *et al.*, 2016). The following enzymes may contribute to the degradation of these components in BDMs: amylases for starch (Pandey *et al.*, 2000), cellulases for cellulosic fibres (Park *et al.*, 2007), and proteases for polylactic acids (PLA) (Oda *et al.*, 2000), correspondingly. In this study, we focused on biodegradable aliphatic and aliphatic-aromatic *co*-polyesters, major materials in commercial BDMs. This biodegradable material can be hydrolytically degraded by microbial enzymes called esterases (Maeda *et al.*, 2005; Shinozaki *et al.*, 2013; Wallace *et al.*, 2017). Thus, esterase activity appears to be useful as an indicator of the biodegradation of polyester-based BDMs in soils.

In studies that measured the activity of esterases that hydrolyse BDMs, *p*NP fatty acids were used as substrates. Moreover, *p*NP fatty acids with various acyl chain lengths have generally been used as substrates to characterize esterases. For example, Wallace *et al.* (2017) reported that an esterase, which was isolated from the

bacterium *Pseudomonas pseudoalcaligenes*, could degrade poly(butylene terephthalate-*co*-adipate) (PBAT) and most strongly hydrolysed *p*NP-C4 as the *p*NP fatty acid substrate. Shinozaki *et al.* (2013) reported that an esterase from the fungus *Pseudozyma antarctica* could hydrolyse various biodegradable aliphatic polyesters and preferentially degraded *p*NP-C5 in the tested *p*NP fatty acid substrate. Thus, microbial esterases that can hydrolyse biodegradable polyesters have different substrate specificities for *p*NP fatty acids. Our previous study reported that the hydrolytic activity of *p*NP-C5, which is associated with the isolation rates of PBSA-degrading fungi, did not correlate with PBSA-degradation rates in 11 cultivated soils (Yamamoto-Tamura *et al.*, 2015). Sander (2019), however, suggested that the lack of correlation was due to a broad set of soil hydrolysis activities of *p*NP-C5, including non-specificity for PBSA degradation. Furthermore, Sakai *et al.* (2002) showed that *p*NP-C2 was useful as an indicator of biodegradation of poly(butylene succinate) (PBS) aliphatic polyesters in field soil. Although these reports show that the hydrolytic activity of these *p*NP substrates is associated with the degradation of biodegradable polyesters composed mainly of single components, the feasibility of using *p*NP-C2 and other *p*NP fatty acids to evaluate the biodegradation of commercial BDMs is yet to be tested in cultivated fields.

This study aimed to select useful *p*NP fatty acid(s) as specific indicator(s) of the microbial activity associated with the biodegradation of PBSA and commercial polyester-based BDMs in cultivated field soil, based on the hydrolytic activity of the *p*NP substrates using the mesh bag method.

## Materials and methods

### Experimental design and mesh bag study

The study was conducted at the Kanagawa Agricultural Technology Center, Japan (35°20' N, 139°16' E), from 8<sup>th</sup> August 2019 to 16<sup>th</sup> March 2020. PBSA film (kindly provided by Unyck Co., Ltd., Tokyo, Japan) (thickness: 15.0±1.3 µm), and two commercial BDMs, hereafter described as films A and B, (thickness: 10.5±1.5 µm and 13.0±1.6 µm, respectively) were used. Based on preliminary <sup>1</sup>H nuclear magnetic resonance (NMR) using deuterated chloroform (CDCl<sub>3</sub>) solution, more than half of the polymer composition in both commercial films was poly(butylene terephthalate-*co*-adipate) (PBAT), with the remainder being PBS-type polymers. Only film B contained PLA at very low ratios. These two commercial films were weathered by covering the same field cropping soybean for 3 months (from 18<sup>th</sup> April 2019 to 23<sup>rd</sup> July 2019) to simulate the actual degradation of mulch films ploughed in the soil after use. The PBSA film was not weathered because of its high biodegradability. All films were stored at 4°C for approximately 2 weeks until use.

The experimental setup is shown in Figure 1. The films were cut into 7×7 cm pieces, weighed, and inserted into envelopes made of non-biodegradable polyester meshes (mesh bags) with 950 µm openings (TB20, NBC Meshtec Inc., Tokyo, Japan). A sewing machine was used to stitch the edges of each bag to prevent spillage. Triplicates for each film were prepared for each sampling time. These mesh bags were buried in the field soil at a depth of 7 cm and then retrieved after 13 d (21<sup>st</sup> August 2019), 33 d (10<sup>th</sup> September 2019), 62 d (9<sup>th</sup> October 2019), 91 d (7<sup>th</sup> November 2019), 152 d (7<sup>th</sup> January 2020), and 221 d (16<sup>th</sup> March 2020). Each mesh bag with soil was kept separately in a plastic bag after removing excess soil.

At each sampling time, 0-15 cm of bulk soil was sampled from points adjacent to where the mesh bags were buried. After retrieval from the field, the mesh bags and the bulk soil samples were transported in a cold box ( $<10^{\circ}\text{C}$ ) to a laboratory at the Institute for Agro-Environmental Sciences, NARO, Tsukuba, Japan, then stored in a refrigerator at  $4^{\circ}\text{C}$  until analysis 2 weeks later.

Temporal changes in soil temperature ( $^{\circ}\text{C}$ , at a depth of 15 cm in the field) and moisture (volumetric water content, at a depth of 10 cm in the field) during the experiment were continuously measured using an RTR-502L sensor and recorder (T&D Corp., Matsumoto, Japan) for soil temperature, and Em50 data logger (Meter Japan, Inc., Koshigaya, Japan) with 5TE sensor (Meter Japan, Inc.) for moisture.

## Sample analyses

### Degradation of buried films

The soil within and adhering to each mesh bag was carefully collected using a toothbrush, and the stitched edges of the retrieved

mesh bags were opened using scissors to remove the films from the mesh bags. Then, the soil adhering to each film coupon and tiny particles of mechanically disintegrated films smaller than the mesh openings ( $<950\ \mu\text{m}$ ) were carefully collected and pooled together. Each pooled soil sample was merged with each soil collected from the outer side of the mesh bags as described above. The bulk soils were carefully mixed and sieved through a 2 mm mesh. All soil samples were stored at  $4^{\circ}\text{C}$  until an esterase activity assay was performed. The films were gently cleaned with distilled water and inserted between plastic lamination films ( $100\ \mu\text{m}$  thickness; KOKUYO, Co., Ltd., Osaka, Japan). The film sets were then air-dried for two weeks at room temperature (around  $25^{\circ}\text{C}$ ). After drying, the lamination films enveloping the biodegradable films were heat-sealed using a laminating machine. The laminated films were scanned using a photo scanner (DS-G20000, Seiko Epson Corp., Suwa, Japan), and the figure files were saved in TIFF format (300 dpi) to evaluate the area loss of the buried films. Compared with a fresh film's  $7\times 7\ \text{cm}$  area, each residual film area in the lamination films was measured based on binarisation with Image J 1.52a soft-

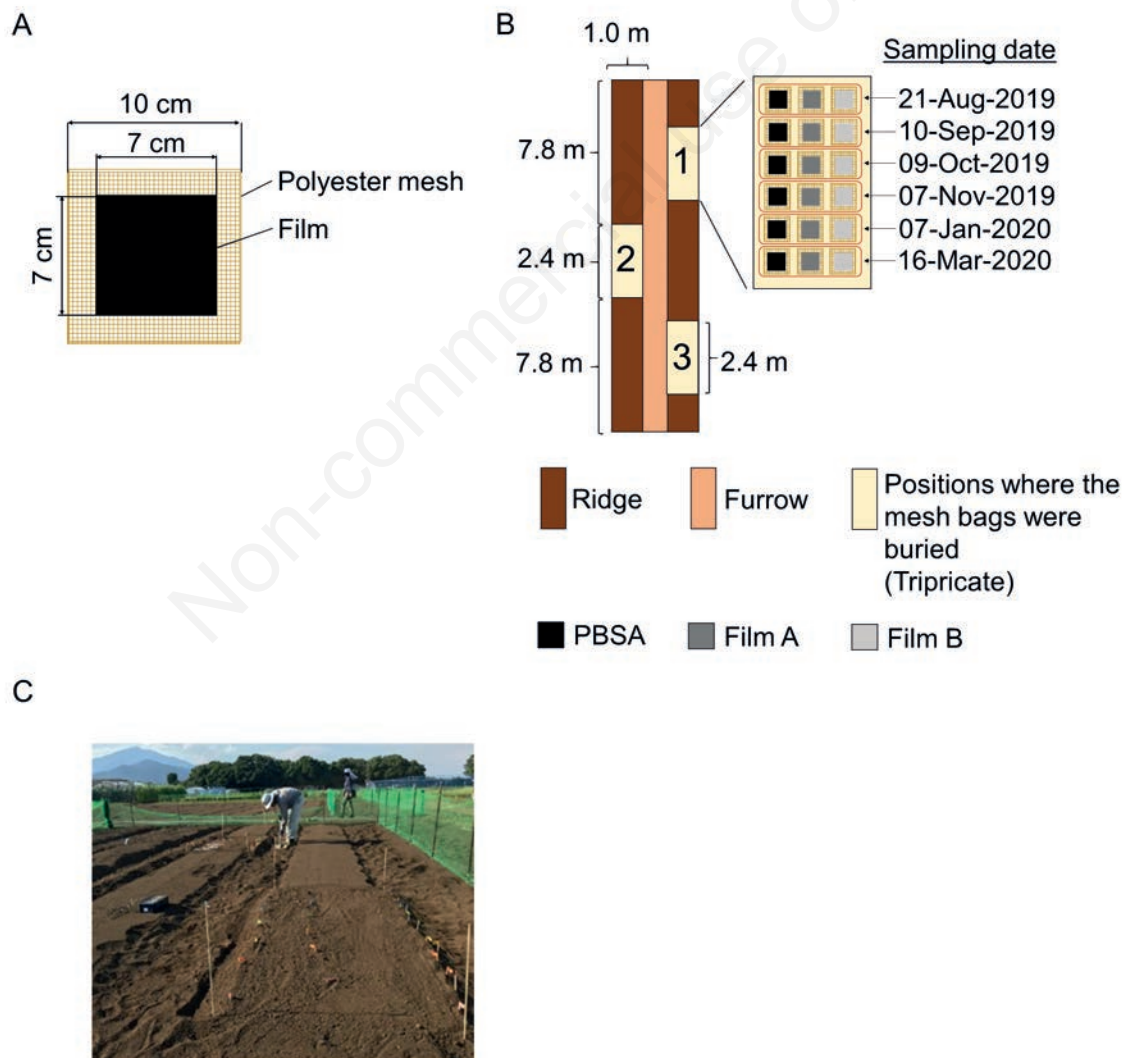


Figure 1. Preparation of mesh bags and field setup. Manufacturing mesh bags (A), the field's setup (B), and a photograph of the field after burying the sets of the bags (C).

ware (National Institutes of Health, USA). The area loss (%) was calculated using the following equation:

$$\text{Area loss (\%)} = \frac{(\text{Average of area of fresh film in triplicate}) - (\text{Area of residual film})}{\text{Average of area of fresh film in triplicate}} \times 100.$$

Based on the extent of the area loss, the temporal change in the area loss of the films can be briefly categorized into three degradation phases, as explained in the results section.

The film degradation was also evaluated as a decrease in the film weights:

$$\text{Weight loss (\%)} = \frac{(\text{Weight of film before burial}) - (\text{Weight of residual film})}{\text{Weight of film before buried}} \times 100$$

### Esterase activity of soils around mesh bags

Soil esterase activity was measured according to Tsuboi *et al.* (2018). Briefly, each soil sample (10–20 mg) was mixed with a reaction buffer [final conc. 10 mM tris(hydroxymethyl) aminomethane (Tris)-maleic buffer, pH 6.0] containing a *p*NP fatty acid. After 30 min incubation at 1500 r min<sup>-1</sup> and 30°C on a shaker (M·BR-022UP, TAITEC Co. Ltd, Saitama, Japan), -80 °C ethanol was added to the reaction container to stop unwanted enzymatic reactions. Then, the soil slurry with cold ethanol was centrifuged at 3000 × *g* at 4°C for 5 min, the supernatant was transferred to a 96-well plate, and cold 2 M Tris was added on ice. The absorbance of the solution was measured at 405 nm using a microplate spectrometer (Benchmark Plus, Bio-Rad Laboratories, Hercules, CA, USA). To measure the hydrolytic activity of soil esterases for esters with different chain lengths, *p*NP-C2, *p*NP-C4, *p*NP-C6, *p*NP-C10, and *p*NP-C12 were used as a substrate independently. *p*NP-C6 was purchased from Tokyo Chemical Industry Co., Ltd. (Tokyo, Japan), and other *p*-nitrophenyl fatty acids were from Sigma-Aldrich (St. Louis, MO, USA).

### Statistical analyses

Statistical analyses were conducted using the “R” statistics software (R Development Core Team, version 4.0.4). First, significant differences among the coefficients of variance of the soil hydrolytic activity calculated for each substrate for each sampling period were evaluated based on the Steel-Dwass test ( $P < 0.05$ ). The difference in esterase activity in each film was statistically evaluated using the Tukey-Kramer test ( $P < 0.05$ ), based on the respective degradation phases as mentioned in the result section. Finally, the statistical correlation between esterase activity and soil temperature and moisture was calculated using the Pearson test ( $P < 0.05$ ).

## Results

### Change of soil temperature and moisture in the field during the experimental period

Temporal changes in soil temperature (°C) and volumetric water content (%) in the field soil are presented in Figure 2. The daily average soil temperature gradually decreased until 19<sup>th</sup> January 2020 (6.4°C, minimum), starting from 32.8°C on 9<sup>th</sup> August 2019 (maximum). Subsequently, the temperature tended to increase until the end of the experiment on 16<sup>th</sup> March 2020. Meanwhile, the seasonal change in the soil moisture content, ranging from 20.2% on 13<sup>th</sup> August 2019, to 32.6% on 29<sup>th</sup> January 2020, became slightly higher from fall to spring than in summer.

### Degradation of biodegradable films in mesh bags

Visual changes in the biodegradable plastic film coupons retrieved from the mesh bags during the experimental period are presented in Figure 3A. The quantified area loss of the film coupons is shown in Figure 3B. Based on the extent of the area loss, the temporal change in the area loss of the films could be briefly divided into three phases: 0%–10% (phase I, starting phase), 10%–99% (phase II, proceeding phase), and 100% (phase III, terminal phase) (Figure 3A). The degradation of the PBSA film was the highest among the three films. The area loss of the PBSA films reached 8.5% (phase I) and 99.1% (phase II) for 13 and 62 d, respectively. By 62 d, the PBSA films disappeared (phase III). The area loss of films A and B did not reach phase III during the investigation period. The area loss of films A and B reached 3.5% for 62 d and 5.9% for 152 d, respectively (phase I). At the end of the experiment (221 d), the area loss of films A and B were 74.4% and 21.6%, respectively (phase II).

The weight loss of the film coupons and the phase changes did not correspond well with the area loss (Figure 3C). The weights of the remaining PBSA films steadily decreased, and a large portion of the PBSA films was degraded after 62 d. The weight of film A decreased at a constant rate until the end of the experiment (221 d) finally reaching 62.9%. Film B showed a steady weight loss (32.3%) until 152 d, but the weight slightly increased at 221 d compared to values recorded prior to 152 d. This weight gain might be due to the adhesion of the soil particles to film B.

### Esterase activities of soils around PBSA and two commercial films

#### Temporal variation

The weight of the soil around the films from each sampling bag was 5.6±1.6 g (from 21<sup>st</sup> August 2019 to 7<sup>th</sup> January 2020). Temporal variations in the hydrolytic activity of *p*NP-C2, -C4, -C6, -C10, and -C12, which were present in the soil around the films, are presented in Figure 4A-E. In the soil around PBSA films, the maximum activity value in each substrate, which was 959.1 nmol·dry g<sup>-1</sup>·min<sup>-1</sup> in *p*NP-C2, 759.1 nmol·dry g<sup>-1</sup>·min<sup>-1</sup> in *p*NP-C4, 512.5 nmol·dry g<sup>-1</sup>·min<sup>-1</sup> in *p*NP-C6, and 100.4 nmol·dry g<sup>-1</sup>·min<sup>-1</sup> in *p*NP-C10, occurred at 33 d. Finally, these

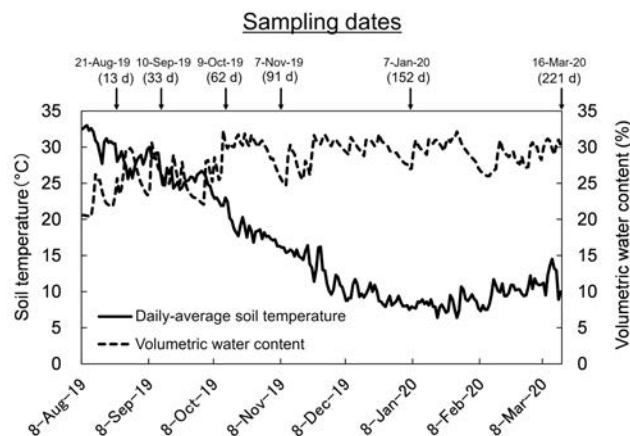


**Figure 2.** Time course of temperature and moisture content in the soil of the experimental field.

activities reached  $292.7 \text{ nmol} \cdot \text{dry g}^{-1} \cdot \text{min}^{-1}$  in *pNP*-C2,  $343.2 \text{ nmol} \cdot \text{dry g}^{-1} \cdot \text{min}^{-1}$  in *pNP*-C4,  $167.0 \text{ nmol} \cdot \text{dry g}^{-1} \cdot \text{min}^{-1}$  in *pNP*-C6, and  $47.4 \text{ nmol} \cdot \text{dry g}^{-1} \cdot \text{min}^{-1}$  in *pNP*-C10 toward the end of the experimental period (221 d: *pNP*-C2, -C4 and -C6; 152 d: *pNP*-C10). For *pNP*-C12, the maximum activity of  $194.9 \text{ nmol} \cdot \text{dry g}^{-1} \cdot \text{min}^{-1}$  was shown at 13 d. After that, the soil hydrolytic activity of *pNP*-C12 decreased and remained constant from 33 to 221 d at a value of  $0 \text{ nmol} \cdot \text{dry g}^{-1} \cdot \text{min}^{-1}$ .

The hydrolytic activities in the soil around films A and B: for *pNP*-C2 was constant at approximately  $500 \text{ nmol} \cdot \text{dry g}^{-1} \cdot \text{min}^{-1}$  until 152 d, then decreased to  $332.9 \text{ nmol} \cdot \text{dry g}^{-1} \cdot \text{min}^{-1}$  in film A, and  $301.0 \text{ nmol} \cdot \text{dry g}^{-1} \cdot \text{min}^{-1}$  in Film B at 221 d (Figure 4A). For *pNP*-C4, the soil hydrolytic activity around film A gradually increased from  $146.0 \text{ nmol} \cdot \text{dry g}^{-1} \cdot \text{min}^{-1}$  at 13 d to  $301.5 \text{ nmol} \cdot \text{dry g}^{-1} \cdot \text{min}^{-1}$  at 221 d, and its maximum value was  $357.0 \text{ nmol} \cdot \text{dry g}^{-1} \cdot \text{min}^{-1}$  at 152 d (Figure 4B). The hydrolytic activity in the soil around film B increased  $178.6 \text{ nmol} \cdot \text{dry g}^{-1} \cdot \text{min}^{-1}$  at 13 d to  $282.5 \text{ nmol} \cdot \text{dry g}^{-1} \cdot \text{min}^{-1}$  at 33 d; and since 33 d, the soil hydrolytic activity around both commercial films remained roughly constant at  $250 \text{ nmol} \cdot \text{dry g}^{-1} \cdot \text{min}^{-1}$  until day 221. For *pNP*-C6, the enzymatic activities in the soils around film A were expected to remain constant, but considerable variation was observed, ranging from  $79.3 \text{ nmol} \cdot \text{dry g}^{-1} \cdot \text{min}^{-1}$  at 91 d to  $253.8 \text{ nmol} \cdot \text{dry g}^{-1} \cdot \text{min}^{-1}$

at 33 d. The soil esterase activity around film B ranged from  $156.9 \text{ nmol} \cdot \text{dry g}^{-1} \cdot \text{min}^{-1}$  at 221 d to  $235.0 \text{ nmol} \cdot \text{dry g}^{-1} \cdot \text{min}^{-1}$  at 91 d and was more constant than those around film A. For *pNP*-C10, the soil hydrolytic activity on films A and B showed the minimum values at 33 d,  $9.6 \text{ nmol} \cdot \text{dry g}^{-1} \cdot \text{min}^{-1}$  and  $36.0 \text{ nmol} \cdot \text{dry g}^{-1} \cdot \text{min}^{-1}$ , respectively (Figure 4D). Since 33 d, these enzymatic activities for *pNP*-C10 in the soils around films A ( $70.9 \text{ nmol} \cdot \text{dry g}^{-1} \cdot \text{min}^{-1}$ ) and B ( $57.2 \text{ nmol} \cdot \text{dry g}^{-1} \cdot \text{min}^{-1}$ ) increased to 152 d, which marked the end of the experimental period. For *pNP*-C12, the hydrolytic activities in the soils around film A remained constant at  $0 \text{ nmol} \cdot \text{dry g}^{-1} \cdot \text{min}^{-1}$  but fell to  $-86.8 \text{ nmol} \cdot \text{dry g}^{-1} \cdot \text{min}^{-1}$  at 62 d (Figure 4E). In the soils around film B, the hydrolytic activities of *pNP*-C12 slightly increased toward 221 d, and the minimum and maximum values were  $-35.3 \text{ nmol} \cdot \text{dry g}^{-1} \cdot \text{min}^{-1}$  at 13 d and  $69.8 \text{ nmol} \cdot \text{dry g}^{-1} \cdot \text{min}^{-1}$  at 152 d. This way, the *pNP*-C12 hydrolysis activities in the soils around both commercial films were below the detection limit during most of the investigation period.

In the bulk field soil, the hydrolytic activities of *pNP*-C2, -C4, -C6, and -C12 were, on average, constant at  $199.8 \text{ nmol} \cdot \text{dry g}^{-1} \cdot \text{min}^{-1}$ ,  $130.6 \text{ nmol} \cdot \text{dry g}^{-1} \cdot \text{min}^{-1}$ ,  $112.9 \text{ nmol} \cdot \text{dry g}^{-1} \cdot \text{min}^{-1}$ , and  $4.7 \text{ nmol} \cdot \text{dry g}^{-1} \cdot \text{min}^{-1}$  for 221 d, respectively. Meanwhile, the hydrolytic activity of *pNP*-C10 was relatively variable and ranged

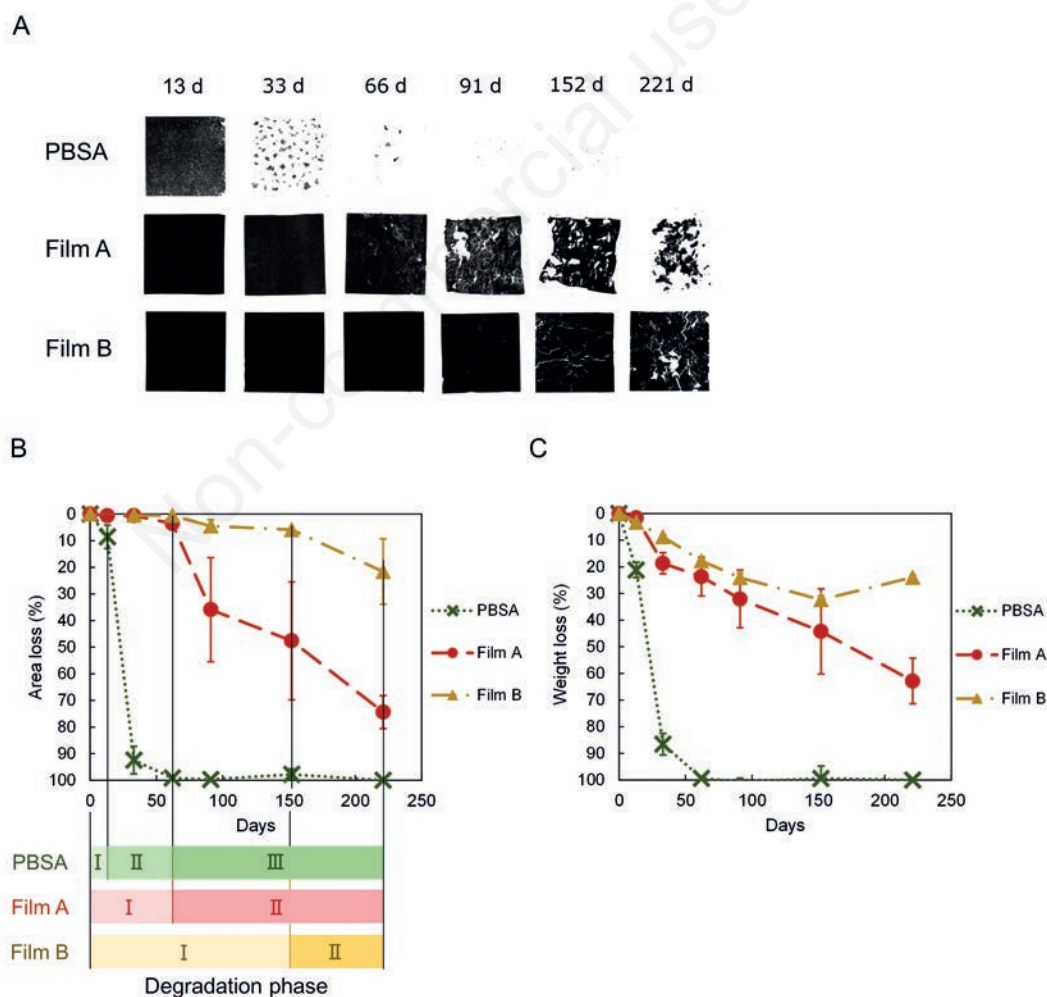


**Figure 3.** Time course of degradation of biodegradable polyester coupons in the mesh bags. Visually (A), area loss (%) (B), and weight loss (%) (C). Bars show standard deviation (SD) among triplicate assays, averaged for three independent reactions.

from  $35.2 \text{ nmol} \cdot \text{dry g}^{-1} \cdot \text{min}^{-1}$  at 13 d to  $0.5 \text{ nmol} \cdot \text{dry g}^{-1} \cdot \text{min}^{-1}$  at 62 d (Figure 4A-E). The coefficients of variance among the enzymatic activities of each substrate in the bulk soil were statistically analysed. The variation in *p*NP-C10 was statistically higher than that of *p*NP-C2, -C4, and -C6 ( $P < 0.05$ ), suggesting that the hydrolytic activity of *p*NP-C10 was not stable when compared with *p*NP-C2, -C4, and -C6.

#### Statistical differences in soil esterase activities around the biodegradable films

The substrates, *p*NP-C2, -C4, and -C6, were subjected to subsequent analyses from the viewpoint of stable measurement of soil esterase activity (Figure 5).

All the values of esterase activity in the soil around the films were statistically higher than those of the bulk soil samples, except for *p*NP-C6 in phase II on film B (Figure 5A-C). Regarding PBSA, the hydrolytic activities of *p*NP-C2, -C4, and -C6 were highest in phase II, the proceeding phase of degradation. In phase III, the terminal phase, these hydrolytic activities in soils around PBSA decreased and approached the values of the bulk soil. The hydrolytic activities of *p*NP-C4 in film A showed differences between phases I and II. On the other hand, in film B, only the hydrolytic activities of *p*NP-C2 could indicate the difference between phases I and II. No statistically significant observations were detected in the substrates showing the highest values in phase II of film B (Tukey-Kramer test,  $P < 0.05$ ).

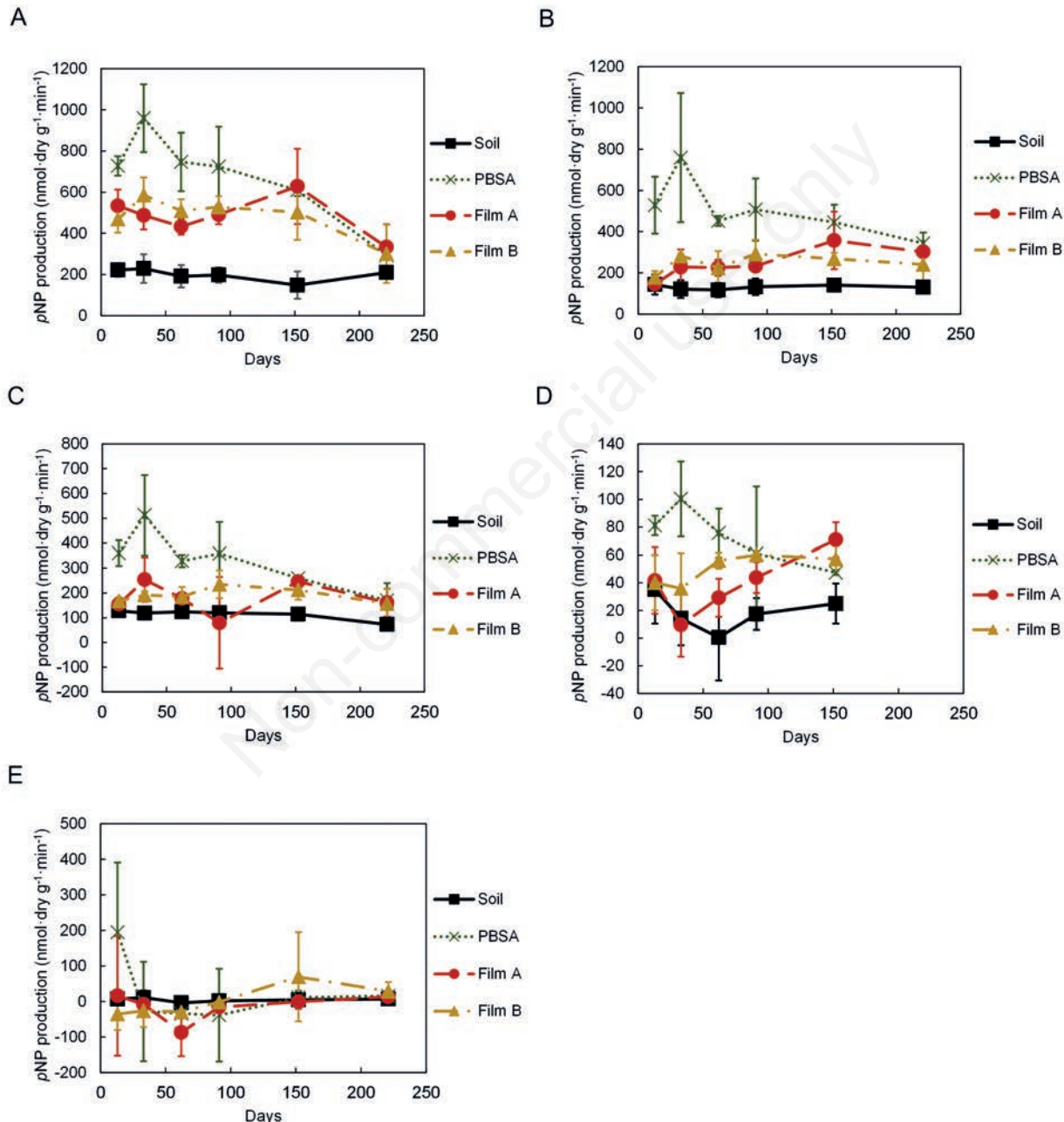


Figure 4. Time course of hydrolytic activities with *p*NP fatty acid substrates. *p*NP-C2 (A), *p*NP-C4 (B), *p*NP-C6 (C), *p*NP-C10 (D), *p*NP-C12 (E). Bars show standard deviation (SD) among ten replicates for bulk soils and three replicates for other soils, averaged for each independent reaction.

### Correlations between the soil temperature, moisture, and esterase activities of the bulk soils

Correlations between the hydrolytic activities of *p*NP-C2, -C4, and -C6 in the bulk soils and the soil temperatures are presented in Figure 6A-C. The hydrolytic activity of *p*NP-C2 ( $R^2=0.66$ ,  $P=0.03$ ) was statistically correlated with soil temperature. The hydrolytic activities of *p*NP-C4 ( $R^2=0.002$ ,  $P=0.93$ ) and -C6

( $R^2=0.51$ ,  $P=0.07$ ) were not correlated with soil temperature.

Correlations between the hydrolytic activities of *p*NP-C2, -C4, and -C6 in the bulk soils and the soil moisture are presented in Figure 6D-F. The hydrolytic activities of *p*NP-C2 ( $R^2=0.16$ ,  $P=0.37$ ) and -C4 ( $R^2=0.45$ ,  $P=0.09$ ) were not significantly correlated with the soil volumetric water content. The hydrolytic activity of *p*NP-C6 negatively correlated with soil moisture ( $R^2=0.62$ ,  $P=0.03$ ).

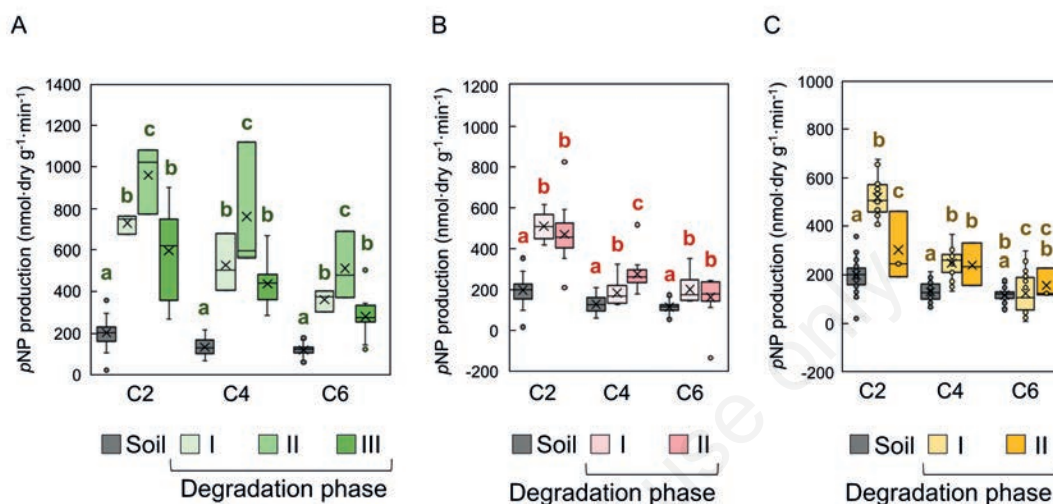


Figure 5. Statistical difference of the hydrolytic activities of *p*NP-C2, -C4, and -C6 among the degradation phases. PBSA (A), film A (B), and film B (C).

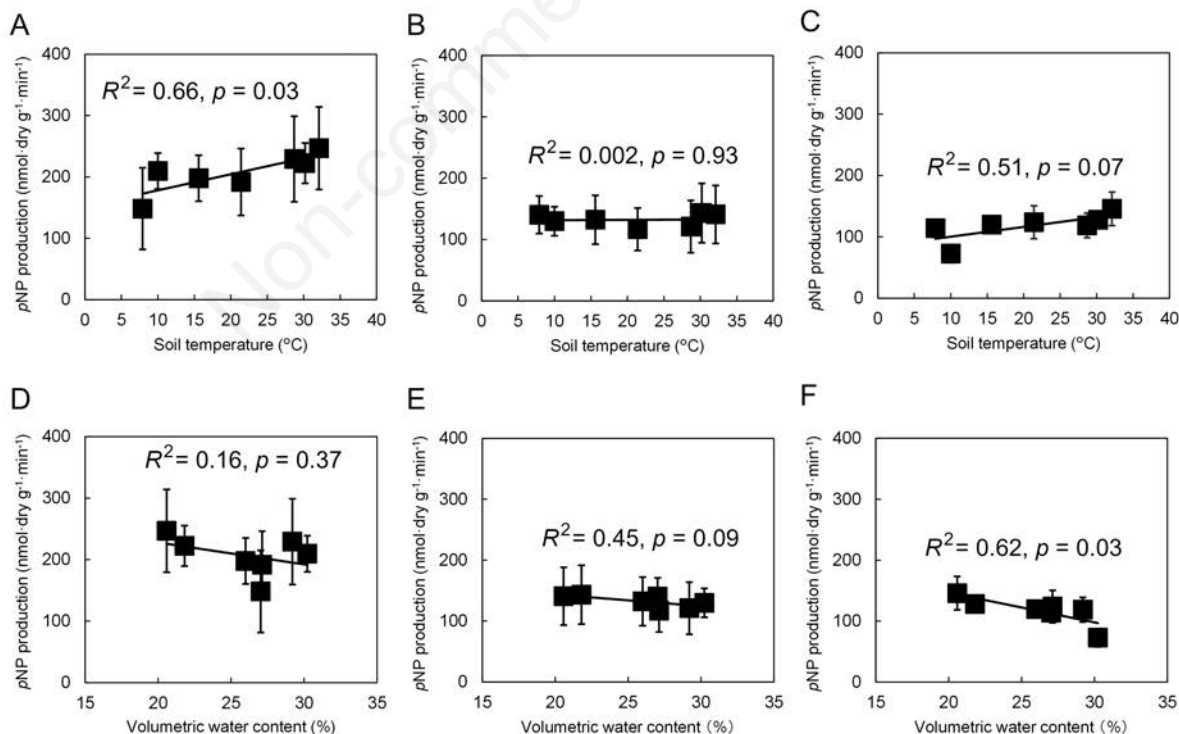


Figure 6. Relations between the hydrolytic activities of *p*NP-C2, -C4, and -C6 and the environmental conditions. *p*NP-C2 vs soil temperature (A), *p*NP-C4 vs soil temperature (B), *p*NP-C6 vs soil temperature (C), *p*NP-C2 vs soil moisture (D), *p*NP-C4 vs soil moisture (E), *p*NP-C6 vs soil moisture (F).

## Discussion

To the best of our knowledge, this is the first study to select a suitable substrate to detect the microbial activity associated with the degradation of biodegradable polyester mulch films based on the time-course of degradation and the hydrolytic activity of several *p*NP fatty acids in the soils of a cultivated field. For this purpose, we have chosen the appropriate substrate from three terms below: the measurement uniformity in replicates among the *p*NP fatty acid substrates, a noticeable increase in the hydrolytic activity (esterase activity) of the substrate during the degradation process, and reactivity according to the degradation of the films and not to the environmental changes (*e.g.*, temperature and moisture).

It is vital to evaluate measurement variances of the hydrolytic activity to select suitable substrate(s). According to Tsuboi *et al.* (2018), the method adopted in the present study demonstrated a low variance in the hydrolytic activity of *p*NP fatty acids in the soil in repetition (Figure 4A-C). However, the hydrolytic activities measured with *p*NP-C10 showed more significant variations than the other substrates, except for *p*NP-C12 ( $P < 0.05$ , Steel-Dwass test) (Figure 4D). The results indicate that the measurements with *p*NP-C10 were unstable and variable in the replicates. The solubility of *p*NP-C10 was lower (10 nM) than that of *p*NP-C4 (0.5 mM) and -C6 (14  $\mu$ M) (Sutton *et al.*, 1990), lower than that of *p*NP-C2. Due to hydrophobic effects, insoluble compounds tend to aggregate in water (Breslow, 1991). Therefore, it might be not easy to dispense the water-based reaction buffer containing the substrate at a uniform concentration because water-insoluble compounds such as *p*NP-C10 do not disperse uniformly in the buffer. This hydrophobicity may lead to variability in the measurement values of hydrolytic activity with *p*NP-C10. The hydrolytic activities of *p*NP-C12 were presented as negative values in part and below the measurement limit in the present study (Figure 4E). The detection limit may be due to its hydrophobicity (0.3 nM) reported by Sutton *et al.* (1990). Thus, the water solubility and hydrolytic degradability of the *p*NP fatty acids may affect the measurement variances in the soil hydrolytic activity of these substrate(s), and they seem to be significant features for consideration to receive reproducible measurements of the hydrolytic activity of *p*NP fatty acids in soils.

Based on the measurement uniformity in replicates, *p*NP-C2, -C4, and -C6 were selected as the candidate substrates in this study. These substrates have also been used to evaluate the hydrolytic activity of microbial enzymes that hydrolyse the biodegradable polyesters PBS and PBSA (Maeda *et al.*, 2005; Shinozaki *et al.*, 2013) and poly(1,4-butylene adipate-co-terephthalate) (PBAT) (Wallace *et al.*, 2017). Previous studies isolated enzymes that can hydrolyse biodegradable polyesters, showing preferential hydrolysis of the acyl chain lengths from *p*NP-C4 to -C6 (Maeda *et al.*, 2005; Shinozaki *et al.*, 2013; Wallace *et al.*, 2017). Thus, *p*NP-C2, -C4, and -C6 could also be used to evaluate the hydrolytic activity of the biodegradable polyesters in soils of cultivated fields.

Among the three degradation phases: phase I (0%-10%), phase II (10%-99%), and phase III (100%), in the soils around both the PBSA film and film A, the hydrolytic activities of *p*NP-C4 were significantly higher in phase II than in other phases (Figure 5A and B). According to a previous report on litter decomposition, enzyme activities change over time in tandem with the degradation of the corresponding component of the litter (Šnajdr *et al.*, 2011). Similarly, our study's hydrolytic activities of *p*NP-C4 may tightly

reflect the degradation of the biodegradable polyesters. However, in the soil around film B, the hydrolytic activities of *p*NP-C4 were not higher in phase II than in phase I (Figure 5C). This may be because the area loss of film B, which presented a very slow degradation rate, reached only 21.6% in phase II at the end of the experiment.

The hydrolytic activities of *p*NP-C2 correlated with soil temperature ( $R^2=0.66$ ,  $P=0.03$ ), and the hydrolytic activities of *p*NP-C6 correlated with moisture ( $R^2=0.62$ ,  $P=0.03$ ) (Figure 6A and F). These results indicate that the activity was variable depending on the environmental conditions. Sakai *et al.* (2002) suggested that the hydrolytic activity of *p*NP-C2 is useful for monitoring the degradation activity of PBS in soil. Our results indicate that the hydrolytic activity of *p*NP-C2 reflected the total microbial activity rather than a specific activity associated with the degradation of the BDMs due to the high correlation with soil temperature. On the other hand, the hydrolytic activities of *p*NP-C4 were not correlated with soil temperature and moisture (Figure 6). These results suggest that the hydrolytic activities of *p*NP-C4 in soils are responsive to the existence of biodegradable polyesters.

The hydrolytic activity of *p*NP-C4 tended to increase as the three films degraded in the soils. At the end of the experiment, in the PBSA, in which pieces of the film were invisible, the hydrolytic activity of *p*NP-C4 gradually decreased towards the baseline value of the activity of the bulk soil, but not to the original activity level (Figure 4B). Similarly, it has been reported that the soil fungal community changed with BDM inoculation, and this change continued after the degradation of solid fragments of the film in our previous study (Sameshima-Yamashita *et al.*, 2019). Thus, the hydrolytic activity of *p*NP-C4 can be used to detect the biodegradation of biodegradable polyesters in soils. Recently, concerns have been raised about the treatment of biodegradable microplastics not to ensure the safety of soil ecosystems (Qin *et al.*, 2015). Our results suggest that the hydrolytic activity of *p*NP-C4 can indicate the biodegradation of biodegradable polyesters, which are difficult to observe visually, from the viewpoint of microbial metabolism in soils. The hydrolytic activity of *p*NP-C4 can also be useful as rapid evidence that polyester-based BDMs will eventually be microbiologically degraded in cultivated field soils, even if it takes a long time for complete degradation.

## Conclusions

The film pieces of PBSA and two commercial BDMs in each mesh bag were buried in the soil of the cultivated field, and the time course of film degradation and the soil hydrolytic activity of *p*NP fatty acids (*p*NP-C2, -C4, -C6, -C10, and -C12) were examined. Among these substrates, *p*NP-C4 was selected as a suitable substrate based on its hydrolytic activity, measurement uniformity between replicates, responsiveness to film degradation, and stability during environmental fluctuations. Even if the films are difficult to observe as degradation proceeds, the hydrolytic activity of *p*NP-C4 can be valuable for detecting the biodegradation of biodegradable polyester mulch films. However, further studies are needed to confirm whether the hydrolytic activity of *p*NP-C4 can be used as a proxy for the microbial activity associated with the degradation of other commercial polyester-based BDMs in other cultivated field locations.

## References

- Bondopadhyay S, Martín-Closas L, Pelacho AM, DeBruyn JM, 2018. Biodegradable plastic mulch films: Impacts on soil microbial communities and ecosystem functions. *Front. Microbiol.* 9:819.
- Breslow R, 1991. Hydrophobic effects on simple organic reactions in water. *Acc. Chem. Res.* 24:159-163.
- Briassoulis D, 2007. Analysis of the mechanical and degradation performances of optimised agricultural biodegradable films. *Polym. Degrad. Stab.* 92:1115-32.
- Francioni M, Kishimoto-Mo AW, Tsuboi S, Hoshino Takada Y, 2022. Evaluation of the mulch films biodegradation in soil: a methodological review. *Ital. J. Agron.* 17:1936.
- Hayes DG, Wadsworth LC, Sintim HY, Flury M, English M, Schaeffer S, Saxton AM, 2017. Effect of diverse weathering conditions on the physicochemical properties of biodegradable plastic mulches. *Polym. Test.* 62:454-67.
- ISO 17556, 2019. Plastics-determination of the ultimate aerobic biodegradability in soil by measuring the oxygen demand in a respirometer or the amount of carbon dioxide evolved. Geneva: ISO.
- Kader MA, Senge M, Mojid MA, Ito K, 2017. Recent advances in mulching materials and methods for modifying soil environment. *Soil Tillage Res.* 168:155-66.
- Li C, Moore-Kucera J, Miles C, Leonas K, Lee J, Corbin A, Inglis D, 2014. Degradation of potentially biodegradable plastic mulch films at three diverse U.S. locations. *Agroecol. Sustain. Food Syst.* 38:861-89.
- Maeda H, Yamagata Y, Abe K, Hasegawa F, Machida M, Ishioka R, Gomi K, Nakajima T, 2005. Purification and characterization of a biodegradable plastic-degrading enzyme from *Aspergillus oryzae*. *Appl. Microbiol. Biotechnol.* 67:778-88.
- Martín-Closas L, Costa J, Pelacho AM, 2017. Agronomic effects of biodegradable films on crop and field environment. In: M. Malinconico (Ed.), *Soil degradable bioplastics for a sustainable modern agriculture*. Springer, Berlin, Germany, pp 67-104.
- Miles C, DeVetter L, Ghimire S, Hayes DG, 2017. Suitability of biodegradable plastic mulches for organic and sustainable agricultural production systems. *HortSci.* 52:10-15.
- Moreno MM, González-Mora S, Villena J, Campos JA, Moreno C, 2017. Deterioration pattern of six biodegradable, potentially low-environmental impact mulches in field conditions. *J. Environ. Manage.* 200:490-501.
- Ngouajio M, Auras R, Fernandez RT, Rubino M, Counts JW, Kijchavengkul T, 2008. Field performance of aliphatic-aromatic copolyester biodegradable mulch films in a fresh market tomato production system. *Horttech.* 18:605-10.
- Oda, Y, Yonetsu, A, Urakami, T, Tonomura K, 2000. Degradation of polylactide by commercial proteases. *J. Polym. Environ.* 8:29-32.
- Pandey A, Nigam P, Soccol CR, Soccol VT, Singh D, Mohan R, 2000. Advances in microbial amylases. *Biotechnol. Appl. Biochem.* 31:135-52.
- Park S, Venditti RA, Abrecht DG, Jameel H, Pawlak JJ, Lee JM, 2007. Surface and pore structure modification of cellulose fibers through cellulase treatment. *J. App. Polymer Sci.* 103:3833-9.
- Qin M, Chen C, Song B, Shen M, Cao W, Yang H, Zeng G, Gong J, 2021. A review of biodegradable plastics to biodegradable microplastics: Another ecological threat to soil environments? *J. Clean. Prod.* 312:127816.
- Sakai Y, Isokawa M, Masuda T, Yoshioka H, Hayatsu M, Hayano K, 2002. Usefulness of soil p-nitrophenyl acetate esterase activity as a tool to monitor biodegradation of polybutylene succinate (PBS) in cultivated soil. *Polym. J.* 34:767-74.
- Sameshima-Yamashita Y, Ueda H, Koitabashi M, Kitamoto H, 2019. Pretreatment with an esterase from the yeast *Pseudozyma antarctica* accelerates biodegradation of plastic mulch film in soil under laboratory conditions. *J. Biosci. Bioeng.* 127:93-8.
- Sander M, 2019. Biodegradation of polymeric mulch films in agricultural soils: Concepts, knowledge gaps, and future research directions. *Environ. Sci. Technol.* 53:2304-15.
- Shinozaki Y, Kikkawa Y, Sato S, Fukuoka T, Watanabe T, Yoshida S, Nakajima-Kambe T, Kitamoto HK, 2013. Enzymatic degradation of polyester films by a cutinase-like enzyme from *Pseudozyma antarctica*: surface plasmon resonance and atomic force microscopy study. *Appl. Microbiol. Biotechnol.* 97:8591-8.
- Sintim HY, Bary AI, Hayes DG, Wadsworth LC, Anunciado MB, English ME, Bandopadhyay S, Schaeffer SM, DeBruyn JM, Miles CA, Reganold JP, Flury M, 2020. In situ degradation of biodegradable plastic mulch films in compost and agricultural soils. *Sci. Total Environ.* 727:138668.
- Šnajdr J, Cajthaml T, Valášková V, Merhautová V, Petránková M, Spetz P, Leppänen K, Baldrian P, 2011. Transformation of *Quercus petraea* litter: successive changes in litter chemistry are reflected in differential enzyme activity and changes in the microbial community composition. *FEMS Microbiol. Ecol.* 75: 291-303.
- Sutton LD, Stout JS, Quinn DM, 1990. Dependence of transition-state structure on acyl chain length for cholesterol esterase catalyzed hydrolysis of lipid p-nitrophenyl esters. *J. Am. Chem. Soc.* 112:8398-403.
- Tsuboi S, Tanaka T, Yamamoto-Tamura K, Kitamoto H, 2018. High-throughput method for the evaluation of esterase activity in soils. *J. Microbiol. Met.* 146:22-4.
- Uchida H, Nakajima-Kambe T, Shigeno-Akutsu Y, Nomura N, Tokiwa Y, Nakahara T, 2000. Properties of a bacterium which degrades solid poly (tetramethylene succinate)-co-adipate, a biodegradable plastic. *FEMS Microbiol. Lett.* 189:25-9.
- Wallace PW, Haernvall K, Ribitsch D, Zitzenbacher S, Schittmayer M, Steinkellner G, Gruber K, Guebitz GM, Birner-Gruenberger R, 2017. PpEst is a novel PBAT degrading polyestrase identified by proteomic screening of *Pseudomonas pseudoalcaligenes*. *Appl. Microbiol. Biotechnol.* 101:2291-303.
- Yamamoto-Tamura K, Hiradate S, Watanabe T, Koitabashi M, Sameshima-Yamashita Y, Yarimizu T, Kitamoto H, 2015. Contribution of soil esterase to biodegradation of aliphatic polyester agricultural mulch film in cultivated soils. *AMB Exp.* 5:10.
- Zumstein MT, Narayan R, Kohler HPE, McNeill K, Sander M, 2019. Dos and do nots when assessing the biodegradation of plastics. *Environ. Sci. Technol.* 53:9967-9.